Journal of Microscopy

Journal of Microscopy, Vol. 259, Issue 2 2015, pp. 155–164 doi: 10.1111/jmi.12276
Received 29 December 2014; accepted 19 May 2015

Combining quantitative 2D and 3D image analysis in the serial block face SEM: application to secretory organelles of pancreatic islet cells

A. SHOMORONY*,§, C.R. PFEIFER*,§, M.A. ARONOVA*, G. ZHANG*, T. CAI†, H. XU†, A.L. NOTKINS† & R.D. LEAPMAN*

*National Institute of Biomedical Imaging and Bioengineering, National Institutes of Health, Bethesda, Maryland, U.S.A

†National Institute of Dental and Craniofacial Research, National Institutes of Health, Bethesda, Maryland, U.S.A

Key words. α cells, β cells, serial block face SEM, stereology, pancreatic islets, secretory granules.

Summary

A combination of two-dimensional (2D) and three-dimensional (3D) analyses of tissue volume ultrastructure acquired by serial block face scanning electron microscopy can greatly shorten the time required to obtain quantitative information from big data sets that contain many billions of voxels. Thus, to analyse the number of organelles of a specific type, or the total volume enclosed by a population of organelles within a cell, it is possible to estimate the number density or volume fraction of that organelle using a stereological approach to analyse randomly selected 2D block face views through the cells, and to combine such estimates with precise measurement of 3D cell volumes by delineating the plasma membrane in successive block face images. The validity of such an approach can be easily tested since the entire 3D tissue volume is available in the serial block face scanning electron microscopy data set. We have applied this hybrid 3D/2D technique to determine the number of secretory granules in the endocrine α and β cells of mouse pancreatic islets of Langerhans, and have been able to estimate the total insulin content of a β cell.

Introduction

The new generation of high throughput three-dimensional (3D) volume tissue reconstruction methods based on scanning electron microscopy (SEM), such as serial block face SEM (SBF-SEM) (Denk & Horstmann, 2004; Briggman *et al.*, 2011; Hoppa *et al.*, 2012; Helmstaedter *et al.*, 2013; Hughes *et al.*, 2013; Pinali *et al.*, 2013; Pfeifer *et al.*, 2014; Young *et al.*, 2014), and focused ion beam SEM (FIB-SEM; Bennett *et al.*, 2009; Hekking *et al.*, 2009; Schneider *et al.*, 2010; Drobne, 2013), provides very large data sets that can be used to build quantitative models of tissue architecture. For example, in SBF-SEM, it is straightforward to acquire 3D volumes that contain $4k \times 4k \times 2k = 0.32 \times 10^{11}$ voxels, and as many as $8k \times 8k \times 4k = 0.25 \times 10^{12}$ voxels. Large data sets of this size present a challenge for the segmentation of cellular ultrastructure. Recently, automated segmentation approaches have been developed that incorporate interactive machine learning in order to recognize features and patterns, including for example the Elastic software package (Kreshuk *et al.*, 2011, 2014; Sommer *et al.*, 2011). These methods have been applied successfully to detect and segment neuronal synapses in brain tissue. Nevertheless, automated segmentation methods are not yet widely available and are more difficult to use than simpler manual segmentation. We have therefore explored a simpler practical approach for handling large SBF-SEM data sets based on combining analyses of segmented 3D volumes with statistical analyses of randomly selected 2D planes within the full 3D data set. The 2D analyses can be considered as a 'virtual stereological' approach, which is readily testable because the entire 3D volume is available. We have used our method to quantify the number of secretory granules and other organelles in cells of mouse islets of Langerhans, which are small endocrine organs distributed throughout the pancreas, comprising several types of secretory cells and associated microvasculature (Brissova *et al.*, 2005; Cabrera *et al.*, 2006; Carter *et al.*, 2009; Kharouta *et al.*, 2009; Steiner *et al.*, 2010).

To illustrate the difficulty in analysing the entire ultrastructural volume of a pancreatic islet, consider a single islet β cell containing approximately 10 000 secretory granules that package the glucose-regulating hormone insulin. In our experience, the task of counting the granules within just one β cell can take more than a day, and the task of measuring the total

§These authors contributed equally to the article.
Correspondence to: Dr. Richard D. Leapman, National Institute of Biomedical Imaging and Bioengineering National Institutes of Health Building 13, Room 3N17 13 South Drive Bethesda, MD 20892, U.S.A. Tel: +1-301-496-2599; fax: +1-301-435-4699; e-mail: leapmanr@mail.nih

volume of the insulin-containing dense cores in all secretory granules of a single β cell takes several days for an experienced operator. Since each islet contains several hundreds of β cells, the time required to analyse manually all $\sim 10^7$ secretory granules within an islet would be prohibitive (Pfeifer *et al.*, 2014).

However, other measurements on the 3D data set can be made much more rapidly. For example, the task of measuring the volume V_{cell} of a cell only requires drawing the boundary of the plasma membrane and measuring the enclosed areas in a series of x–y block face views. Having determined the 3D volume of a cell from the full SBF-SEM data set, it is then possible to determine the total number of secretory granules in that cell from estimates of the number of granules per unit volume. Such measurements of granule number density can be obtained either by applying a stereological approach to analyse randomly selected 2D block face views throughout the cell, or by selecting a number of subvolumes and counting the number of granules within each. As we shall see later, it is necessary to make corrections for granule-deficient regions of the cell such as the nucleus, mitochondria, and Golgi.

Materials and methods

Specimen preparation

Pancreatic islets from 2- to 3-month-old male mice were prepared as described previously (Zhang *et al.*, 2007; Cai *et al.*, 2011) with all procedures approved by the NIDCR Institutional Animal Care and Use Committee.

To prepare specimens for SBF-SEM, we employed a heavy metal staining protocol, which has been developed by Dr. Mark Ellisman's laboratory at the University of California, San Diego, CA, U.S.A. (West *et al.*, 2010; Holcomb *et al.*, 2013). Initially, isolated islets were fixed for 5 min in a mixture of 2.5% glutaraldehyde and 2% formaldehyde in sodium cacodylate buffer containing 2 mM calcium chloride. Fixation was then continued for an additional 2–3 h on ice using the same solution, after which the samples were rinsed three times, each for 5 min, with cold cacodylate buffer containing 2 mM calcium chloride.

To stain the islets with heavy metal, they were fixed for 1 h on ice in a solution of Reduced Osmium, consisting of 3% potassium ferrocyanide in 0.3 M cacodylate buffer, 4 mM calcium chloride and 4% aqueous osmium tetroxide. The samples were then placed in a 0.22 μm-Millipore-filtered 1% thiocarbohydrazide solution in double-distilled water for 20 min. After this step had been completed, the samples were fixed in 2% osmium tetroxide in double-distilled water for 30 min. The samples were then placed in 1% aqueous uranyl acetate solution and left overnight at a temperature of 4°C. Finally, after washing the samples with double-distilled water five times, each for 3 min, they were stained en bloc with Walton's lead aspartate (Walton, 1979), and placed in the oven for 30 min. After another five 3-min rinses in double-distilled water, the samples were dehydrated and embedded in Epon–Araldite according to a standard protocol.

SBF-SEM

To perform SBF-SEM, it was necessary to mount the epon-embedded block in the specimen stage of the SEM in such a way as to minimize electrical charging of the block by the electron beam. Each block of the embedded islets was first mounted on top of an empty resin block that could be trimmed by an ultramicrotome (Leica Ultracut). After exposure of the islet and the heavy metal stain, the block was remounted with the exposed islet turned downwards and glued using CW2400 Conductive Epoxy (Circuit Works), so that it was in electrical contact with an aluminium specimen pin (Gatan, Pleasanton, CA, U.S.A.). The remounted block was then trimmed again to expose the other side of the islet and then sputter-coated with a thin layer of gold.

The epon-embedded, stained blocks were imaged using a 3View serial block-face imaging system (Gatan) installed on a Zeiss SIGMA-VP (variable pressure) SEM, operating in high-vacuum mode at an accelerating voltage of 1.5 kV using a 30 μm condenser aperture. Block face image series were collected with a pixel size of 5.4 nm in the x–y plane with successive removal of 25 nm slices perpendicular to the z-axis, and a pixel dwell time of 1.5 μs and a probe current of approximately 40 pA. Resulting 3D data sets were aligned using the Digital Micrograph software (Gatan) and were uploaded into the Amira software (FEI Inc., Hillsboro, OR, U.S.A.) for 3D visualization and quantitative analysis. Further processing of 2D images was performed using Image software (Schneider *et al.*, 2012).

Determining total numbers of dense core granules by segmenting cellular compartments

We shall show that the measured numbers of dense core granules per unit volume ρ_{gran} that are contained within granule-rich cytoplasmic subvolumes of pancreatic islet cells of a given type, that is, α or β cells, and within the same islet, are distributed about a mean value with a relatively small standard error of around 5%. Furthermore, we find that such measurements of ρ_{gran} can be made from relatively small numbers of randomly selected 3D volumes or 2D images in islet cells. Importantly, in the SBF-SEM technique, assumptions about the variation in numbers of dense cores per unit volume can easily be tested within a data set. On the other hand, the task of determining the total numbers of dense core granules per cell requires knowledge of the total cell volume, which cannot easily be determined from randomly selected 2D TEM images. For example, it is often impossible to determine from randomly selected 2D images whether different cells have a narrow or wide distribution of total cellular volumes. However, SBF-SEM enables us to perform rapid and precise segmentation of individual cell volumes, as well as segmentation of major subcellular

compartments that are distinct from the granule-rich regions of cytoplasm. Meanwhile, we can still use a statistical approach to determine the numbers of the populous secretory granules per unit volume, without having to segment all $\sim 10^4$ granules in a single cell. This combined technique therefore allows us to estimate the total number of secretory granules per cell much more rapidly and more accurately than can be done by applying a conventional stereological approach to TEM images.

To determine the total number of dense core secretory granules in a cell, we consider the cell volume that is available to the granules, which is equal to the total cell volume V_{cell} after subtraction of the volumes of other compartments $V_{\text{comp(n)}}$ that do not contain granules, such as the nucleus, mitochondria, and extended regions of Golgi:

$$N_{\text{gran}} = \rho_{\text{gran}} \left[V_{\text{cell}} - \sum_{1}^{n} V_{\text{comp(n)}} \right]. \quad (1)$$

With this approach, there is no need to consider compartments such as endoplasmic reticulum, which permeate throughout cytoplasmic regions rich in secretory granules because those compartments are already reflected in the number of dense core granules per unit volume ρ_{gran} in Eq. (1). We can determine ρ_{gran} directly by analyzing granule-rich subvolumes or 2D subareas, as described below.

Measurement of islet cell and organelle volumes

The volumes of pancreatic α and β cells V_{cell} were determined by tracing around the plasma membrane at all n planes at depths z_n in the block, where the cell was located. If the z-increment between planes is Δz, then the cell volume is given by

$$V_{\text{cell}} = \sum_{n} \Delta z \iint_{\text{cell}(z_n)} dx\, dy. \quad (2)$$

Similarly, the volumes of the α and β cell nuclei V_{nuc} were determined by tracing around the nuclear membrane at all n planes at depths z_n in the block where the nucleus was located:

$$V_{\text{nuc}} = \sum_{n} \Delta z \iint_{\text{nuc}(z_n)} dx\, dy. \quad (3)$$

Since mitochondria exhibited higher contrast than all the other subcellular organelles, the mitochondrial volume could be determined by using the threshold function in the Amira software. This provided a volume fraction of mitochondria f_{mit} in the cell. It was observed, however, that the mitochondrial-rich regions of the cell excluded more secretory granules than would be expected based purely on the mitochondrial volume. This observation can be explained by the close spacing of branched mitochondria, which tended to prevent access to granules. The effective volume fraction of mitochondria f'_{mit} is therefore given by $f'_{\text{mit}} = f_{\text{mit}}\ \gamma_{\text{mit}}$, where γ_{mit} is a factor by which the mitochondrial volume is increased to take into account the exclusion of secretory granules. The value of γ_{mit} can be estimated by analysing 2D cellular regions that are rich in mitochondria.

We considered the endoplasmic reticulum to be distributed throughout the 3D subvolumes and 2D block face views used to determine the secretory granule number density. Golgi apparatus was not prominent in the β cells but there were distinct regions of this organelle in the α cells. These Golgi volumes were segmented and analysed by the Amira software to give a volume fraction f_{Golgi} in the cell.

Measurement of secretory granule number density

The number density of secretory granules in α and β cells was determined (1) by stereological analysis of 2D sections through the cells, and (2) by counting granules in 3D subvolumes of the cell.

In the stereological approach, we analysed five granule-rich areas of size 2 μm $\times$ 2 μm in SBF-SEM planes, taken at roughly even intervals throughout the β cell. Here, granule-rich areas were defined as regions outside the cell nucleus that were absent of mitochondria in the case of β cells, and absent of mitochondria and Golgi in the case of α cells. Since all α and β cell granules contain dense cores of packaged glucagon and insulin, respectively, granules were counted only if their dense cores were visible in the selected planes. Most β cell secretory granules exhibit wide halos, possibly associated with the processing of the precursor protein, proinsulin. Although such structures could be readily identified as secretory granules, they were only counted if their dense cores were evident. The number of granules contained within each region was determined as follows: any dense core residing wholly within the square was counted as one granule, whereas any partially enclosed dense core was counted as one-half of a granule. This provided an estimate of the number of secretory granules per unit area n_{gran}. From the number of dense cores in each granule-rich square, the number of granules per unit volume, that is, the number density ρ_{gran}, could be determined from

$$\rho_{\text{gran}} = \frac{n_{\text{dense core}}}{D_{\text{dense core}} + d}, \quad (4)$$

where $D_{\text{dense core}}$ is the average diameter of the granule's dense core, and d is the thickness of the slab from which the image is recorded (Loud, 1968). In the thick-slab limit when $d \gg D_{\text{dense core}}$, Eq. (4) reduces to the standard formula for converting number per unit area to number per unit volume by dividing by the specimen thickness. However, when $d \ll D_{\text{dense core}}$, the denominator in Eq. (4) compensates for the over-counting since a dense core appears in several consecutive sections.

In the subvolume analysis method, five boxes were extracted from randomly selected granule-rich regions throughout the

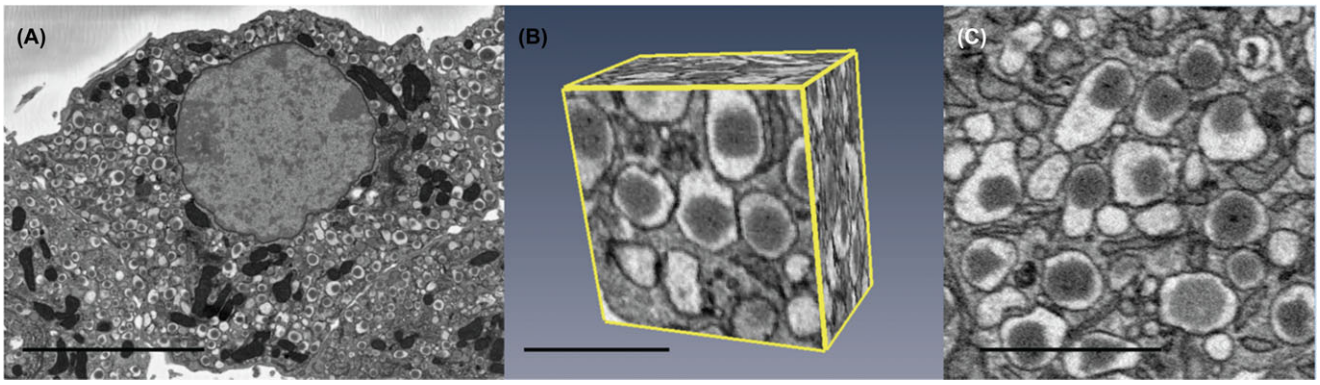

Fig. 1. Different methods for finding the packing density of a β cell: (A) 100-nm-thick (pseudo-TEM) thin section. Bar = 5 μm. (B) Representation of a 3D box used for granule counting; note that the actual boxes used in this work measured 1 μm × 1 μm × 1.5 μm. Bar = 1 μm. (C) 25-nm-thick "flat area." Bar = 1 μm.

3D visualization of the α and β cells. The numbers of granules were counted manually within each box, once again counting fully and partially enclosed granules as whole granules and half-granules, respectively.

Both the 2D stereological method and the 3D subvolume method provided measurements of ρ_{gran}, from which a mean and standard deviation could be computed for each method. Representative SBF-SEM data in Figure 1 show a 100 nm pseudo-TEM thin section of a β cell obtained by summing four consecutive block face images (Fig. 1A), a 3D subvolume used to count secretory granules (Fig. 1B), and a single 25-nm-thick slab through a granule-rich cellular region revealing the angular facets of the crystalline dense cores (Fig. 1C).

Determination of number of secretory granules per cell

By taking into account the excluded volumes of nuclei, mitochondria, and Golgi (for α cells), we can write expressions for the numbers of secretory granules in the two cell types.

The average number of secretory granules in an α cell is given by

$$N_{\alpha\ \text{gran}} = \rho_{\alpha\ \text{gran}}[V_{\alpha\ \text{cell}}(1 - f'_{\alpha\ \text{mit}}) - V_{\alpha\ \text{nuc}} - V_{\alpha\ \text{Golgi}}], \quad (5)$$

and the average number of secretory granules in a β cell is given by

$$N_{\beta\ \text{gran}} = \rho_{\beta\ \text{gran}}[V_{\beta\ \text{cell}}(1 - f'_{\beta\ \text{mit}}) - V_{\beta\ \text{nuc}}]. \quad (6)$$

We also counted the precise number of secretory granules in a particular selected β cell by summing groups of four consecutive SBF-SEM images, separated by 25 nm, to yield approximately 100 'pseudo-TEM' serial thin sections of thickness $d = 100$ nm, as illustrated in Fig. 1A.

Measurement of granule dense core volume

The insulin content of β cells could be estimated from the volume fraction of secretory granule dense cores contained within randomly selected regions that are rich in secretory granules. In this analysis, the volume sampled by single 2D block face images is considered to be representative of the 3D volume of the granule rich regions in the β cell. Granule-rich regions of size 1.5 μm × 1.5 μm were selected, and for each region the dense cores were segmented and the area fraction $f_{\text{dense core}}$ of the dense cores, equal to the volume fraction, was determined. These measurements could be related to the total insulin mass packaged in the secretory granules of β cells by excluding the volumes of the nucleus and mitochondria. The mass of insulin per mass of β cells is given by

$$\frac{m_{\text{insulin}}}{m_{\beta\ \text{cell}}} = f_{\text{dense core}} \cdot \left[\frac{\rho_{\text{insulin}}}{\rho_{\beta\ \text{cell}}}\right] \cdot \left[1 - \frac{V_{\text{nuc}}}{V_{\beta\ \text{cell}}} - f'_{\beta\ \text{mit}}\right], \quad (7)$$

and the average mass of insulin per β cell is given by

$$m_{\text{insulin}} = V_{\beta\ \text{cell}} \cdot \rho_{\text{insulin}} \cdot f_{\text{dense core}} \cdot \left[1 - \frac{V_{\text{nuc}}}{V_{\beta\ \text{cell}}} - f'_{\beta\ \text{mit}}\right], \quad (8)$$

where ρ_{insulin} is the density of the crystallized form of insulin that is contained in the dense cores of the secretory granules, and $\rho_{\beta\ \text{cell}}$ is the density of a β cell. Estimates of the insulin density can be obtained from the crystal structure of insulin, which is reported in the literature.

Results and discussion

Comparison of methods for determining number of secretory granules in β cell

We have compared three approaches for determining the number of secretory granules in a β cell. We began our analysis by measuring the precise volume of a particular randomly selected cell by contouring the plasma membrane in successive SBF-SEM block face images (Fig. 2A). Next, we determined the volumes of cellular organelles that were excluded from secretory granules, that is, the nucleus and mitochondria. The endoplasmic reticulum and Golgi were interspersed in the granule-rich regions of the β cells, so they did not need to

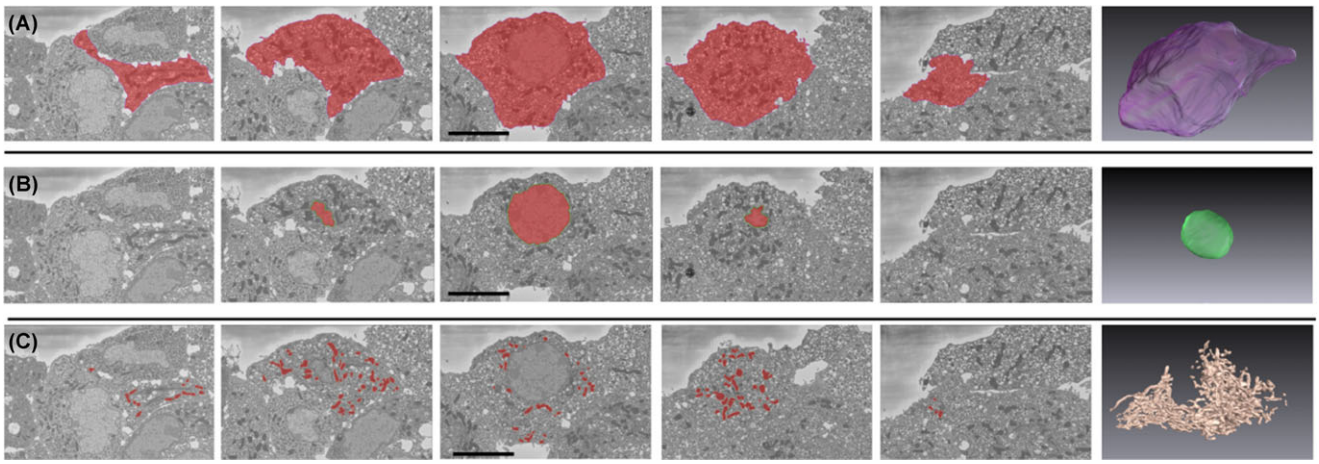

Fig. 2. Determination of the volume available to granules in a β cell: representative block face images in which the operator is segmenting the cell membrane (A), nucleus (B), and mitochondria (C). Calculated nuclear and mitochondrial volumes are subtracted from the total cell volume to yield the volume available for granule-packing. Bars = 5 μm. Results of the analysis are presented in Table 1.

Table 1. Parameters used to determine numbers of secretory granules in β cells of mouse pancreatic islet. Measurements of numbers of granules per unit volume were used to estimate the total number of granules in cell #1, for which the granules were counted manually

β-granule parameter	Mean	SD	SEM	n
Number of β-granules per unit area in granule-rich regions of 2 μm × 2 μm images (μm^{-2})	3.98	0.80	0.20	15
Diameter of β-granule core (μm)	0.24	0.042	0.003	212
Number of β-granules per unit volume in granule-rich region obtained from Eq. (4) (μm^{-3})	15.0	3.0	0.8	15
Number of β-granules per unit volume in granule-rich 1 μm x 1 μm x 1.5 μm boxes (μm^{-3})	17.6	1.8	–	5
Volume fraction of β-cell nucleus	0.129	0.022	–	20
Volume fraction of mitochondria in β-cell	0.077	0.021	–	6
Correction factor for mitochondrial excluded volume	2.05	0.74	–	8
Mean volume of β-cell (μm^3)	930	140	–	30
Mean number of β-granules per cell after correction for nuclear and mitochondrial volumes	9,950	1,500	–	15
Volume of selected cell#1 (μm^3)	1,010	30[a]	–	–
Estimated number of β granules in cell #1	10,800	–	–540	15
Measured number of β granules in cell #1 by manual counting in full 3D SBF-SEM data set	11,700	100[b]	–	–

[a]Standard deviation estimated from 10 different measurements of same cell
[b]Standard deviation estimated from uncertainty in identifying β-granules

be treated separately. The nuclear volume was determined by tracing the outer nuclear membrane in successive block face images, in the same way as the cell membrane (Fig. 2B). The plasma membrane, nucleus and mitochondria are also shown as surface-rendered representations in Fig. 2A–C, respectively. Analysis of 20 such β cells gave a ratio of nuclear volume to cell volume of $V_{\mathrm{nuc}}/V_{\beta\ \mathrm{cell}} = 0.129 \pm 0.022$ (standard deviation). Analysis of mitochondria in six β cells gave a ratio of mitochondrial volume to cell volume of $f_{\beta\ \mathrm{mit}} = 0.077 \pm 0.021$ (standard deviation). Since the mitochondria stained more strongly than every other organelle, including secretory granule dense-cores, it was possible to determine the total mitochondrial volume by thresholding the voxel intensities of the entire cell using the Amira software (Fig. 2C). We also found it necessary to apply a correction factor γ_{mit} as described in the Methods section to take account of additional excluded volume associated with the mitochondria. Measurements of eight mitochondrial-rich regions gave a value of $\gamma_{mit} = 2.05 \pm 0.74$ (standard deviation). This resulted in a value of $f'_{\beta\ \mathrm{mit}} = f_{\beta\ \mathrm{mit}}\ \gamma_{\beta\ \mathrm{mit}} = 0.159 \pm 0.058$ (standard deviation) and a s.e.m. of 0.021.

We first applied a stereological approach on granule-rich areas of β cells on a single block face image through the islet to determine the number of secretory granule dense-cores per unit volume $\rho_{\beta\ cell}$ based on Eq. (4). This estimation required knowledge of the mean dense-core diameter, which has previously been determined as 240 ± 42 nm (Pfeifer *et al.*, 2014), as well as β cell volume measurements and the fractional volume occupied by the nucleus and mitochondria, as indicated in Table 1. We also analysed five granule-rich subvolumes of the β cell to measure directly the number of granules per unit volume, as described in the Materials and Methods section. The

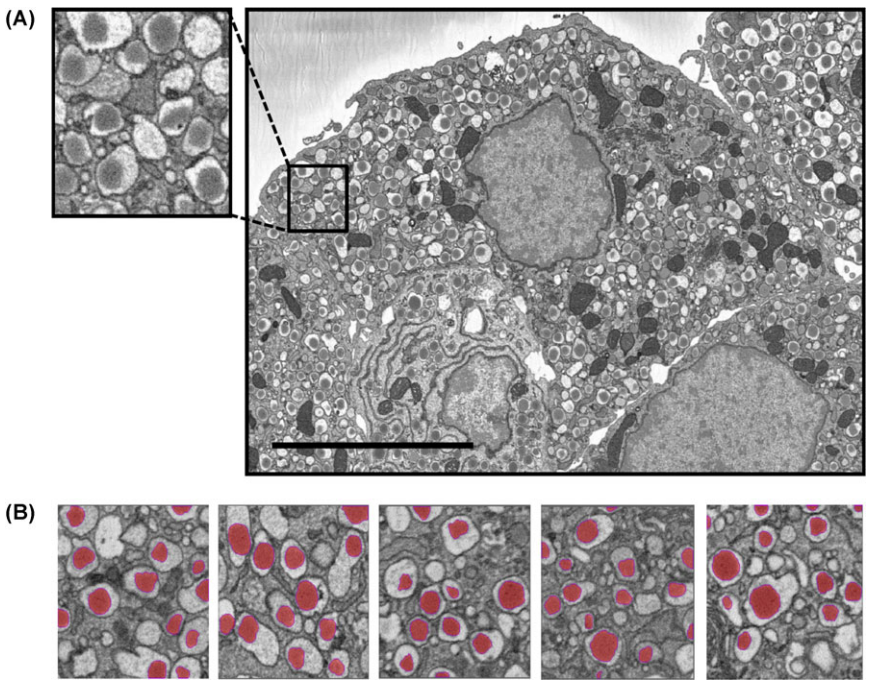

Fig. 3. Determination of the total volume of secretory granule dense-cores in β cell. Subimages of size 1.5 μm x 1.5 μm within a β cell (A) are imported into Amira (or ImageJ) and their dense-cores are manually segmented (B).

results of these volume measurements were consistent with those obtained from the 2D stereological measurements to within the experimental error (Table 1). Finally, we used this statistical approach to estimate the number of secretory granules within a particular β cell (cell #1 in Table 1), for which we know the number of secretory granules to high accuracy and precision based on manual counting from the complete SFB-SEM data set. Manual counting indicated that there are 11 700 $\pm$ 100 secretory granules in cell #1, compared with 10 800 $\pm$ 540 (s.e.m.) obtained from stereological analysis of the 2D images, which shows reasonable agreement. This discrepancy of 8% is mainly attributed to systematic errors in determining the mean dense core diameter, from which the number of secretory granules per unit volume is determined using Eq. (4). Nevertheless, Table 1 shows that cells with larger volumes (e.g., cell #1) contain more secretory granules than cells with smaller volumes. Our results are also consistent with values obtained from serial section electron tomography of β cells in rapidly frozen, freeze-substituted mouse islets (Noske *et al.*, 2008). We believe that the 8% difference between the number of β granules obtained from our combined stereological and volume measurement approach, and the number obtained by precise counting all granules in a particular β cell, is acceptable since it is smaller than the 14% standard deviation in the cellular volumes of the β cell population (Table 1). The variations between numbers of granules in different β cells can therefore be mainly attributed to variations in the cellular volume available to the secretory granules.

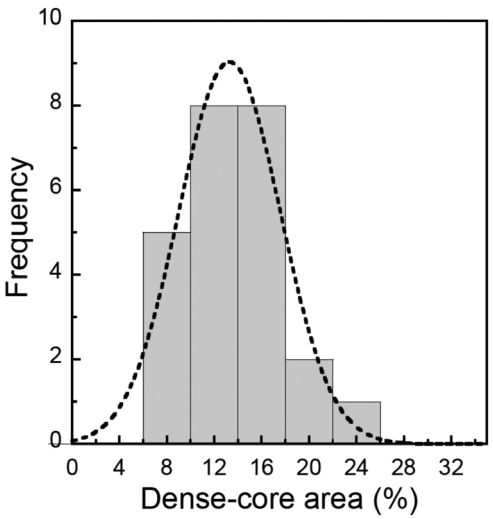

Fig. 4. Analysis of 24 granule-rich regions of β cells in mouse pancreatic islet: the percentage of block-face area occupied by the insulin-containing dense-cores is plotted as a histogram.

Estimated insulin content of β cells based on dense core volume fraction

It is known that the dense cores of β-cell secretory granules consist almost entirely of the hormone insulin, which regulates blood glucose levels. Ultrastructural evidence for this includes the observation that the dense cores frequently have angular crystalline facets, as illustrated in Fig. 1C. Insulin

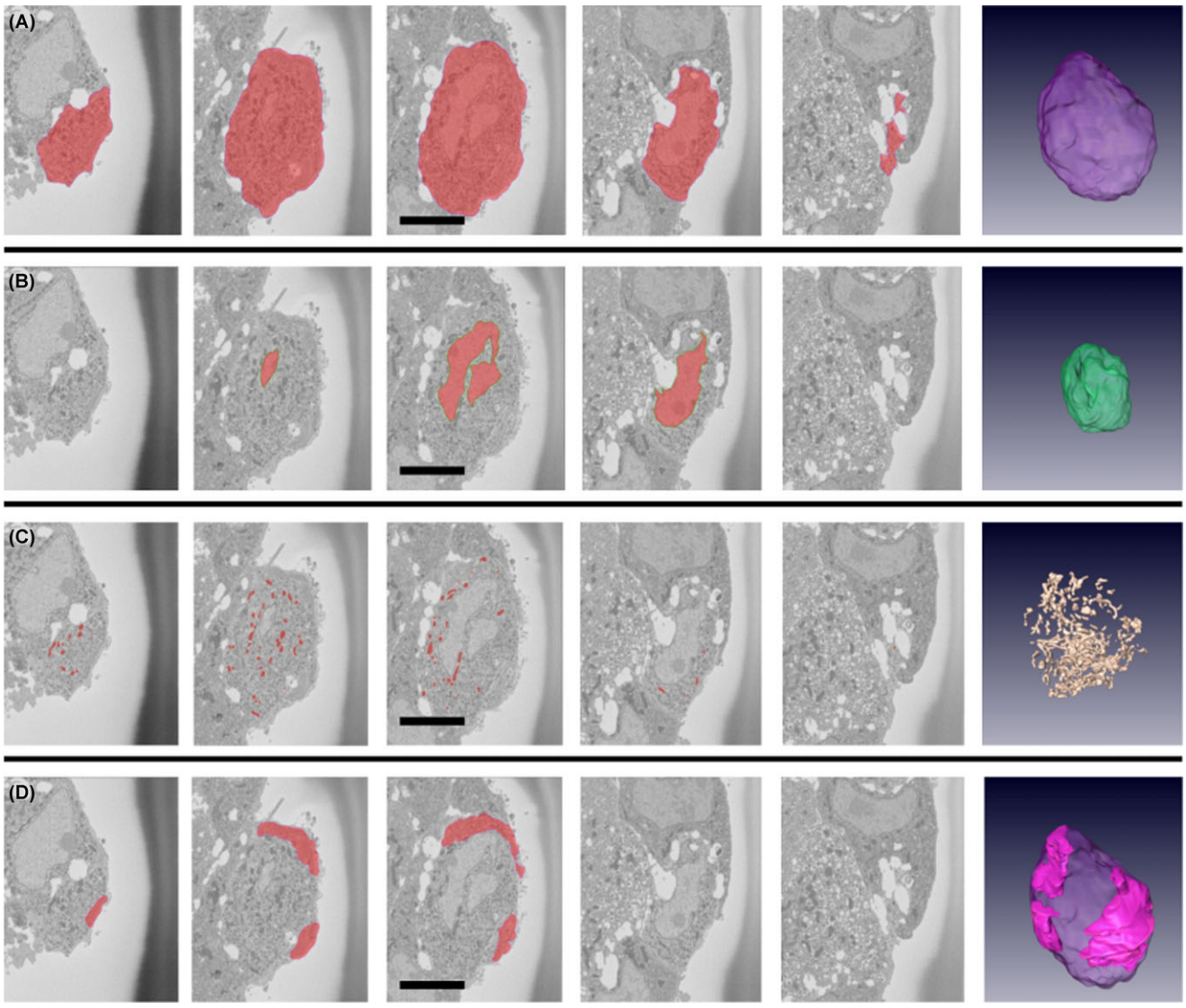

Fig. 5. Determination of the volume available to granules in a α cell: representative block face images in which the operator is segmenting the cell membrane (A), nucleus (B), mitochondria (C), and a Golgi-rich region (D). The calculated nuclear, mitochondrial and ER-rich-region volumes are subtracted from the total cell volume to yield the volume available for granule-packing. Bars = 5 μm. Results of the analysis are presented in Table 2.

across all vertebrate species contains 51 amino-acids with six cysteine residues, that is, ~12% of the amino-acids contain sulphur (Conlon, 2000). The sulphur content of insulin is therefore about three times higher than for typical proteins in the Swiss Protein Data Base. Indeed, analysis of the dense cores by electron energy loss spectroscopy (EELS) reveals that the sulphur-to-nitrogen ratio has an unusually high value of 0.087 ± 0.015:1 (Goping *et al.*, 2003), which is consistent with the value of 0.097:1 for pure insulin (Leapman & Ornberg, 1988). If we assume that the protein crystals in the granule dense cores do not shrink during specimen preparation, we can estimate the total mass of insulin in the β cell from the dense-core volume throughout the cell and the crystal density. Although we do not know the precise crystal structure of insulin in the dense-cores of pancreatic islet β cells, we can obtain an estimate from crystallographic measurements on reconstituted insulin. For example, Badger and Caspar report the structure of cubic insulin crystals with unit cell dimension $a = 78.9$ Å containing 24 insulin molecules per unit cell, with a molecular mass of 5778 Da (Badger & Caspar, 1991; Badger *et al.*, 1991). This gives a dry density for the insulin crystal of 0.47 g cm^{-3}.

The volume fraction of dense cores in β cells was estimated by segmenting the dense cores in randomly selected granule-rich areas of size 1.5 μm × 1.5 μm or 1.0 μm × 1.0 μm using the NIH ImageJ software, and by measuring the fraction of the area that they occupy. Five of these areas are illustrated in Figure 3, where the dense cores are coloured red, and analysis

Table 2. Parameters used to determine numbers of secretory granules in α cells of mouse pancreatic islet

α-granule parameter	Mean	SD	SEM	*n*
Number of α-granules per unit area in granule-rich regions of 1 μm × 1 μm images (μm^{-2})	8.65	1.46	0.30	30
Diameter of α-granule core (μm)	0.23	0.058	0.004	215
Number of α-granules per unit volume in granule-rich region obtained from Eq. (4) (μm^{-3})	33.9	5.7	1.5	15
Volume fraction of α-cell nucleus	0.250	0.024	–	20
Volume fraction of α-cell Golgi	0.087	0.040	0.008	–
Volume fraction for mitochondria	0.037	0.008	–	6
Mean volume of α-cell (μm^3)	520	120	–	30
Mean number of α-granules per cell after correction for nuclear, mitochondrial and Golgi volumes	10,400	2,400	–	15

of all 10 regions is presented in Table 1. By analysing 24 images in granule-rich regions of β cells, it was found that 13.2% ± 2.7% (standard deviation) of the image areas consisted of dense-core material, as shown by the histogram in Figure 4. Applying the same excluded volume factors that were used to determine the number of secretory granules in the β cell in Eq. (6), we estimate that the mass of insulin per gram of β cells is 0.045 g ± 0.010 g (standard deviation). For a typical β cell volume of 930 μm^3, we can therefore estimate that each cell contains about 42 pg of insulin. Our estimates of insulin mass per mass of β cells obtained from the total measured volume of β granule cores is consistent with biochemical measurements such as those by Declercq *et al.* on β cells from two genetically modified mouse models, which report values of 100 μg of insulin for 4 mg of mouse β cells (i.e., 0.025 g per gram of β cells), and 350 μg of insulin for 7 mg of mouse β cells (i.e., 0.050 g per gram of β cells; Declercq *et al.*, 2010). The insulin content is also consistent with early biochemical assays of the dry mass fraction of insulin in β cells extracted from rabbit islets (Lacy & Williamson, 1962). These authors determined that the dry mass fraction of insulin in rabbit islet β cells is 0.145 ± 0.015, which corresponds to 0.043 ± 0.005 g of insulin per hydrated gram of β cells assuming β cells have a water content of 70%.

Determination of number of secretory granules in α cell

Having demonstrated that a 2D stereological approach combined with 3D volume measurements can be used to determine the number of secretory granules in β cells of pancreatic islets, we now apply the same approach to determine the number of secretory granules in the glucagon-secreting α cells. A cells have smaller volumes than β cells but their nuclei are almost the same size as β cell nuclei. The secretory granules in α cells have much thinner halos so their overall diameter is only about half of that of the β cell. In addition to regions that are rich in mitochondria, α cells also contain extended regions of Golgi that are separated from the secretory granule-rich regions. In our analysis, we therefore needed to consider the Golgi as another organelle that excluded secretory granules.

Figure 5 shows segmentation of ultrastructure in an α cell at five different SBF-SEM planes including: the plasma membrane, which gives the total cell volume (Fig. 5A), the nucleus (Fig. 5B), the mitochondria (Fig. 5C), and the Golgi (Fig. 5D). Each of these structures is also illustrated by a surface rendered model.

The number of α granules per unit volume was determined from stereological analysis of fifteen 1 μm × 1 μm granule-rich regions. Using the excluded volume corrections indicated in Table 2, we were able to determine the number of glucagon-secreting α granules per cell. Our analysis revealed that each α cell contains 10 400 ± 2400 secretory granules. This value is higher than previous values obtained by González-Vélez *et al.* (2012), who estimate the mouse α cells contain ~5800 secretory granules based on rough geometrical estimates of the α cell volume, and granule number density. Our measurements show that although the α cell volume is only about half that of a β cell, the α cell contains almost as many secretory granules. This result is also evident from the more than double packing density of secretory granules in α cells relative to β cells, despite the similar dense-core diameters for the two granule types. A higher packing density of secretory granules in α cells is facilitated by the smaller halos surrounding the dense-cores compared with the much large halos of the β granules.

Conclusion

It is possible to obtain accurate and consistent quantitative measurements from 3D ultrastructure acquired using serial block face SEM without having to analyse entire datasets. Precise measurements of large but irregular ultrastructural volumes can be made quickly because relatively small numbers of contours need to be drawn and segmented. For example, it is straightforward to trace the plasma membrane or nuclear membrane of a cell. In contrast, it is very time-consuming to contour and segment large numbers of small organelles within the entire 3D volume of a cell. On the other hand, small structures can often be efficiently analysed by a stereological approach based on statistical sampling of randomly selected 2D areas that are typical of those found throughout the cell or subregions of the cell. However, it is very difficult to use a stereological approach to obtain accurate information from

large structures, such as the volumes of whole cells or nuclei, without making assumptions, which are often invalid, about their shapes and size distribution. This is because there are often too few of the large structures available for analysis in randomly selected 2D planes.

We have demonstrated the advantage of combining a full 3D segmentation of large structures, for example, the entire plasma membrane and nucleus, together with a stereological or statistical analysis of smaller structures. We have applied this approach to obtain quantitative measurements on secretory granules in pancreatic islets, including the numbers of secretory granules in α and β cells, as well as to deduce the insulin content of the β cell. There is considerable interest in determining the phenotype of pancreatic islets at the level of individual cells. For example, type two diabetes is characterized by defective insulin secretion, as well as atypical glucagon secretion, associated with changes in islet function and islet mass (Rosengren *et al.*, 2012; Brereton *et al.*, 2014). Literature values for the volumes of α and β cells and the total number of secretory granules in each cell type vary quite widely mainly because reported values have depended on a purely stereological approach (Olofsson *et al.*, 2002; Straub *et al.*, 2004; Fava *et al.*, 2012), rather than a stereological approach combined with precision measurements using SBF-SEM, as reported here. The SBF-SEM approach offers higher accuracy and precision in determining the numbers of secretory granules not only in cells of the pancreatic islet but also in many other secretory cells that are associated with diseases of the endocrine and exocrine systems.

Acknowledgments

This work was supported by the Intramural Research Program of the National Institute of Biomedical Imaging and Bioengineering, and the National Institute of Dental and Craniofacial Research, NIH.

References

Badger, J. & Caspar, D.L.D. (1991) Water-structure in cubic insulin crystals. *Proc. Natl. Acad. Sci. U.S.A.* **88**, 622–626.

Badger, J., Harris, M.R., Reynolds, C.D., Evans, A.C., Dodson, E. J., Dodson, G.G. & North, A.C.T. (1991) Structure of the pig insulin dimer in the cubic crystal. *Acta. Crystallogr. B.* **47**, 127–136.

Bennett, A.E., Narayan, K., Shi, D., Hartnell, L.M., Gousset, K., He, H.F., Lowekamp, B.C., Yoo, T.S., Bliss, D., Freed, E.O. & Subramaniam, S. (2009) Ion-abrasion scanning electron microscopy reveals surface-connected tubular conduits in HIV-infected macrophages. *PloS Pathogens* **5**(9): e1000591. doi: 10.1371/journal.ppat.1000591.

Brereton, M.F., Iberl, M., Shimomura, K., Zhang, Q., Adriaenssens, A.E., Prok, P., Spiliotis, I.I., Dace, W., *et al.* (2014) Reversible changes in pancreatic islet structure and function produced by elevated blood glucose. *Nat. Commun.* **5**, 4639. doi: 10.1038/ncomms 5639/www.nature.com/naturecommunications.

Briggman, K.L., Helmstaedter, M. & Denk, W. (2011) Wiring specificity in the direction-selectivity circuit of the retina. *Nature* **471**, 183–188.

Brissova, M., Fowler, M.J., Nicholson, W.E., Chu, A., Hirshberg, B., Harlan, D.M. & Powers, A.C. (2005) Assessment of human pancreatic islet architecture and composition by laser scanning confocal microscopy. *J. Histochem. Cytochem.* **53**, 1087–1097.

Cabrera, O., Berman, D.M., Kenyon, N.S., Ricordi, C., Berggren, P.O. & Caicedo, A. (2006) The unique cytoarchitecture of human pancreatic islets has implications for islet cell function. *Proc. Natl. Acad. Sci. U.S.A.* **103**, 2334–2339.

Cai, T., Hirai, H., Zhang, G., Zhang, M., Takahashi, N., Kasai, H., Satin, L.S., Leapman, R.D. & Notkins, A.L. (2011) Deletion of Ia-2 and/or Ia-2 β in mice decreases insulin secretion by reducing the number of dense core vesicles. *Diabetologia* **54**, 2347–2357.

Carter, J.D., Dula, S.B., Corbin, K.L., Wu, R.P. & Nunemaker, C.S. (2009) A practical guide to rodent islet isolation and assessment. *Biol. Proc. Online* **11**, 3–31.

Conlon, J.M. (2000) Molecular evolution of insulin in nonmammalian vertebrates. *Am. Zool.* **40**, 200–212.

Declercq, J., Kumar, A., Van Diepen, J.A., *et al.* (2010) Increased β-cell mass by islet transplantation and PLAG1 overexpression causes hyperinsulinemic normoglycemia and hepatic insulin resistance in mice. *Diabetes* **59**, 1957–1965.

Denk, W. & Horstmann, H. (2004) Serial block-face scanning electron microscopy to reconstruct three-dimensional tissue nanostructure. *PloS Biol.* **2**, 1900–1909.

Drobne, D. (2013) 3D imaging of cells and tissues by focused ion beam/scanning electron microscopy (FIB/SEM). *Methods Mol. Biol.* **950**, 275–292.

Fava, E., Dehghany, J., Ouwendijk, J., Muller, A., Niederlein, A., Verkade, P., Meyer-Hermann, M. & Solimena, M. (2012) Novel standards in the measurement of rat insulin granules combining electron microscopy, high-content image analysis and in silico modelling. *Diabetologia* **55**, 1013–1023.

Gonzalez-Velez, V., Dupont, G., Gil, A., Gonzalez, A. & Quesada, I. (2012) Model for glucagon secretion by pancreatic α-cells. *PloS One* **7**, e32282.

Goping, G., Pollard, H.B., Srivastava, M. & Leapman, R. (2003) Mapping protein expression in mouse pancreatic islets by immunolabeling and electron energy loss spectrum-imaging. *Microsc. Res. Techniq.* **61**, 448–456.

Hekking, L.H.P., Lebbink, M.N., De Winter, D.A.M., Schneijdenberg, C.T.W.M., Brand, C.M., Humbel, B.M., Verkleij, A.J. & Post, J.A. (2009) Focused ion beam-scanning electron microscope: exploring large volumes of atherosclerotic tissue. *J. Microsc. Oxford* **235**, 336–347.

Helmstaedter, M., Briggman, K.L., Turaga, S.C., Jain, V., Seung, H.S. & Denk, W. (2013) Connectomic reconstruction of the inner plexiform layer in the mouse retina. *Nature* **500**, 168–174.

Holcomb, P.S., Hoffpauir, B. K., Hoyson, M. C., Jackson, D.R., Deerinck, T.J., Marrs, G.S., Dehoff, M., Wu, J., *et al.* (2013) Synaptic inputs compete during rapid formation of the calyx of held: a new model system for neural development. *J. Neurosci.* **33**, 12954–12969.

Hoppa, M.B., Jones, E., Karanauskaite, J., Ramracheya, R., Braun, M., Collins, S.C., Zhang, Q., Clark, A., *et al.* (2012) Multivesicular exocytosis in rat pancreatic β cells. *Diabetologia* **55**, 1001–1012.

Hughes, L., Towers, K., Starborg, T., Gull, K. & Vaughan, S. (2013) A cell-body groove housing the new flagellum tip suggests an adaptation of cellular morphogenesis for parasitism in the bloodstream form of *Trypanosoma brucei*. *J. Cell Sci.* **126**, 5748–5757.

Kharouta, M., Miller, K., Kim, A., Wojcik, P., Kilimnik, G., Dey, A., Steiner, D. F. & Hara, M. (2009) No mantle formation in rodent islets-the prototype of islet revisited. *Diab. Res. Clin. Proc.* **85**, 252–257.

Kreshuk, A., Straehle, C.N., Sommer, C., Koethe, U., Cantoni, M., Knott, G. & Hamprecht, F.A. (2011) Automated detection and segmentation of synaptic contacts in nearly isotropic serial electron microscopy images. *PloS One*, **6**(10): e24899. doi: 10.1371/journal.pone.0024899.

Kreshuk, A., Koethe, U., Pax, E., Bock, D.D. & Hamprecht, F.A. (2014) Automated detection of synapses in serial section transmission electron microscopy image stacks. *PloS One* **9**(2): e87351. doi: 10.1371/journal.pone.0087351.

Lacy, P.E. & Williamson, J.R. (1962) Quantitative histochemistry of islets of langerhans. 2. Insulin content of dissected β-cells. *Diabetes* **11**, 101–104.

Leapman, R.D. & Ornberg, R. L. (1988) Quantitative electron-energy loss spectroscopy in biology. *Ultramicroscopy* **24**, 251–268.

Loud, A.V. (1968) A quantitative stereological description of ultrastructure of normal rat liver parenchymal cells. *J. Cell Biol.* **37**, 27–46.

Noske, A.B., Costin, A.J., Morgan, G.P. & Marsh, B.J. (2008) Expedited approaches to whole cell electron tomography and organelle mark-up in situ in high-pressure frozen pancreatic islets. *J. Struct. Biol.* **161**, 298–313.

Olofsson, C., Gopel, S., Barg, S., Galvanovskis, J., Ma, X., Salehi, A., Rorsman, P. & Eliasson, L. (2002) Fast insulin secretion reflects exocytosis of docked granules in mouse pancreatic β-cells. *Pflug. Arc. Eur. J. Phy.* **444**, 43–51.

Pfeifer, C.R., Shomorony, A., Aronova, M.A., Zhang, G., Cai, T., Xu, H., Notkins, A.L. & Leapman, R.D. (2014) Quantitative analysis of mouse pancreatic islet architecture by serial block-face SEM. *J. Struct. Biol.* **189**, 44–52.

Pinali, C., Bennett, H., Davenport, J.B., Trafford, A.W. & Kitmitto, A. (2013) Three-dimensional reconstruction of cardiac sarcoplasmic reticulum reveals a continuous network linking transverse-tubules this organization is perturbed in heart failure. *Circ. Res.* **113**, 1219–1230.

Rosengren, A.H., Braun, M., Mandi, T., Andersson, S.A., Travers, M.E., Shigeto, M., Zhang, E.M., Almgren, P., *et al.* (2012) Reduced insulin exocytosis in human pancreatic β-cells with gene variants linked to type 2 diabetes. *Diabetes* **61**, 1726–1733.

Schneider, C.A., Rasband, W.S. & Eliceiri, K.W. (2012) NIH image to ImageJ: 25 years of image analysis. *Nature Methods* **9**, 671–675.

Schneider, P., Meier, M., Wepf, R. & Muller, R. (2010) Towards quantitative 3D imaging of the osteocyte lacuno-canalicular network. *Bone* **47**, 848–858.

Sommer, C., Straehle, C., Kothe, U. & Hamprecht, F.A. (2011) Ilastik: interactive learning and segmentation toolkit. In *Proceedings of 8th IEEE International Symposium on Biomedical Imaging: from Nano to Macro*. pp. 230–233. IEEE Catalog Number: CFP11BIS; ISBN: 978-1-4244-4128-0.

Steiner, D.J., Kim, A., Miller, K. & Hara, M. (2010) Pancreatic islet plasticity Interspecies comparison of islet architecture and composition. *Islets* **2**, 135–145.

Straub, S.G., Shanmugam, G. & Sharp, G. W.G. (2004) Stimulation of insulin release by glucose in associated with an increase in the number of docked granules in the β-cells of rat pancreatic islets. *Diabetes* **53**, 3179–3183.

Walton, J. (1979) Lead aspartate, on en-bloc contrast stain particularly useful for ultrastructural enzymology. *J. Histochem. Cytochem.* **27**, 1337–1342.

West, J.B., Fu, Z.X., Deerinck, T.J., Mackey, M.R., Obayashi, J.T. & Ellisman, M.H. (2010) Structure-function studies of blood and air capillaries in chicken lung using 3D electron microscopy. *Respir. Physiol. Neurobiol.* **170**, 202–209.

Young, R.D., Knupp, C., Pinali, C., Png, K.M.Y., Ralphs, J.R., Bushby, A.J., Starborg, T., Kadler, K.E. & Quantock, A.J. (2014) Three-dimensional aspects of matrix assembly by cells in the developing cornea. *Proc. Natl. Acad. Sci. U.S.A.* **111**, 687–692.

Zhang, G., Hirai, H., Cai, T., Miura, J., Yu, P., Huang, H., Schiller, M. R., Swaim, W. D., Leapman, R. D. & Notkins, A. L. (2007) RESP18, a homolog of the luminal domain IA-2 is found in dense core vesicles in pancreatic islet cells and is induced by high glucose. *J. Endocrinol.* **195**, 313–321.

Supporting Information

Additional Supporting information may be found in the online version of this article at the publisher's website:

The complete stack of block face images from β cell #1 analysed in Table 1, together with the surface rendering of the cell's plasma membrane.